

COHERENT STRUCTURES AND ORIGINATION OF POWERFUL SOUND OSCILLATIONS AROUND BLUFF BODIES

S.P. Bardakhanov, M.M. Katasonov

Khristianovich Institute of Theoretical & Applied Mechanics, Siberian Branch of Russian Academy of Sciences, Novosibirsk, Russia

H.J. Sung

Department of Mechanical Engineering, Korea Advanced Institute of Science and Technology, Daejeon, Korea

ABSTRACT

The onset of acoustic resonance in flow around thick plate, cylindrical pipe and circular disk as bluff bodies has been studied. The cylindrical, toroidal and three-dimensional coherent structures shed in the wake. The region of their origination served as a source of acoustic disturbances. At certain range of free-stream velocity the strong amplification of sound arises, because of shedding frequency coincidence with eigen acoustic frequency of flow region.

1. INTRODUCTION

Approaches based on coherent structures (CS) concept are extensively used in turbulence studies since 70's. The potential benefit of such approaches is the possibility of turbulent flow control, because by means of structures' manipulation the whole flow can be altered. In this paper the flow control will be discussed emphasizing the aeroacoustic resonance phenomenon.

For the first time the acoustic resonance phenomenon in a flow near periodic lattice of plates in the rectangular channel, caused by non-stationary separation of a boundary layer at trailing edges of thin plates, was described by Parker (1966). He had shown that oscillations are purely acoustic and not connected to vibrations of plates. The case of the wake behind thick plate was studied by Bardakhanov and Lygdenov (1990). By Sukhinin and Bardakhanov (1998) the complete linear mathematical model had been proposed and compared with experimental data for a case of flat plates. The purpose of this study was to investigate the peculiarities of occurrence of acoustic resonant oscillations in plane, axisymmetric and three-dimensional flow.

Long time ago L.Prandtl showed the unstationary flow dynamics at the separation zone of the bluff body (Figure 1). We claim this zone as the main place where sound-flow interaction occurs (Figure 2). The regions, where the flow separates from the

solid surface is the key region for the active flow control because of instability of this region and of its high receptivity to external disturbances, namely, acoustical ones.

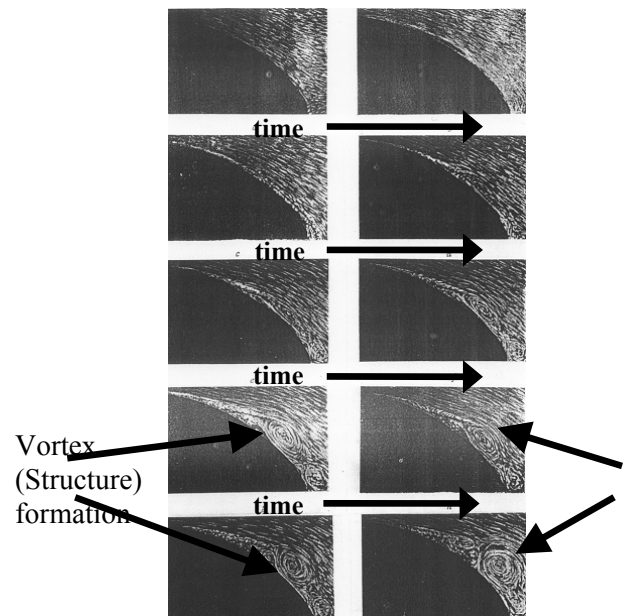


Figure 1: Bluff Body - Flow Near the Trailing Edge (L.Prandtl)

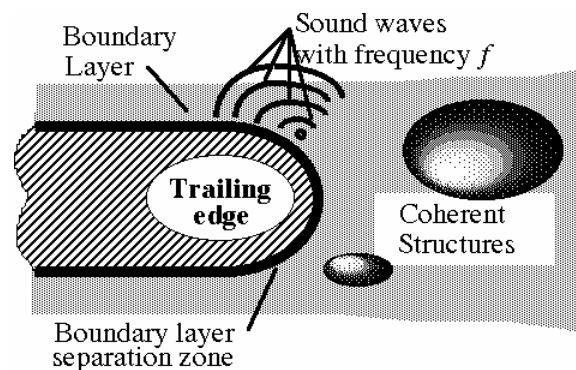


Figure 2: Scheme of sound-flow interaction in vicinity of the wake origination region

Then the following results illustrate the flow

control for aeroacoustic resonance through control of CS originated at trailing edge and connection of changes in CS with general change of the flow parameters.

2. EXPERIMENTAL PROCEDURE

The tests were carried out at Khristianovich Institute of Theoretical and Applied Mechanics, Novosibirsk and Korea Advanced Institute of Science and Technology, Daejeon in subsonic wind tunnels of circuit type with a closed test section. The following models were used: thick plates of length 150÷710 mm of thickness 8-40 mm, axisymmetric tubes of length 150÷400 mm with internal diameter of 84 mm and thickness of a wall 8 mm and disks by a diameter $D = 200$ and 160 mm and thickness of 8 mm. The leading and trailing edges of all models were rounded, but some were blunt and rhombic. The models were installed along a flow (in parallel to the top and bottom walls of a test section).

The free stream velocity U_∞ was measured by Pitot-Prandtl probe and the tests were carried out in a range from 5 up to 40 m/sec. The longitudinal components of mean U and rms velocity u' in flow were measured by hot-wire probe. For the qualitative control of sound pressure level, for the analysis of a sound spectrum, and also as a source of a reference signal a microphones were used.

Alongside with measurements in a boundary layer of the model and in a wake behind it, the measurements of velocity fluctuations in a standing sound wave were carried out. For this purpose the probe was moved along to a flow outside of boundary layers on a model and on walls of a test section at various distances from a model's surface.

3. RESULTS AND DISCUSSION

3.1 Plane case

3.1.1 Sound origination for single plate

Scheme of experiment is presented at Figure 3.

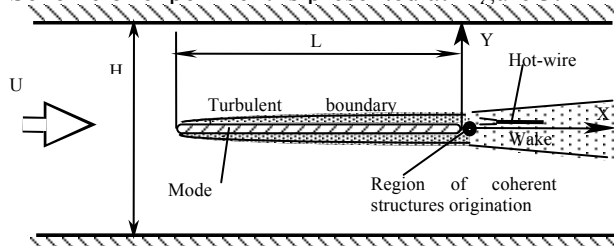


Figure 3: Plane single plate configuration

On all models the CS' shedding was observed at the trailing edge, Figure 4a. Their generation can be suppressed by passive or active control, for instance, by simultaneous excitation from two

acoustic sources with determined difference of phases between them (Figure 4b). The existence of CS is supported by spectra of velocity fluctuations, which contain a component on allocated frequency, superior a level of turbulent background fluctuations. This frequency we call as a main frequency f_0 . It depends linearly on free-stream velocity but at some ranges it keeps constant with the origination of sound, Figure 5. At the resonance the structures are well organized what was shown by experimental data in the wake near the trailing edge (Figure 6).

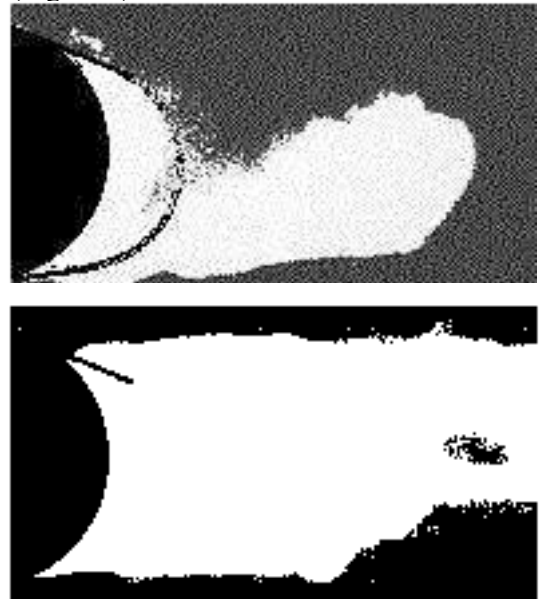


Figure 4: Smoke-wire images – a) vortical CS exists, b) CS is suppressed

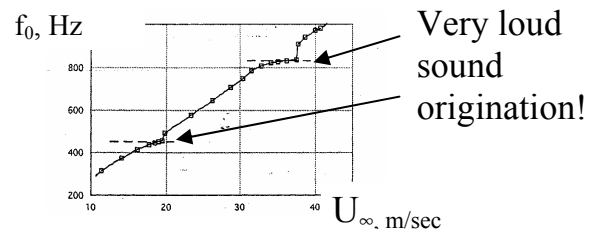


Figure 5: CS shedding frequency vs. free-stream velocity

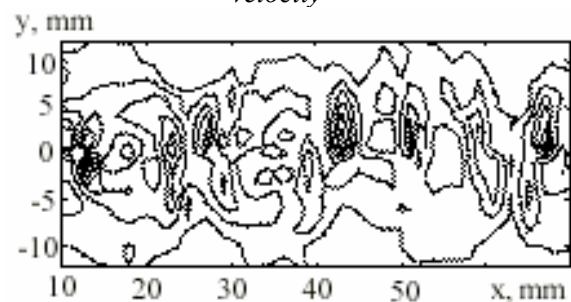


Figure 6: CS shape near trailing edge obtained from experimental data

Based on the received data on onset and development of coherent structures in the wakes after the bluff bodies the researches were continued

on intensively carried out in the seventieth of the phenomenon of an aeroacoustic resonance, namely in conditions, when a source of its excitation are coherent structures.

3.1.2 Sound modulation for two plates system

Two plates were used in configuration presented at Figure 7. Thickness of plate B was slightly larger than thickness of plate A. In this case the dependence of shedding frequency vs. free-stream velocity was different for each plate (Figure 8). The spectra for the numbered ranges are shown at the Figure 9. This system originates different sound frequency or two frequencies at the same time due to transfer of control from one source of resonance to another (from plate A to B).

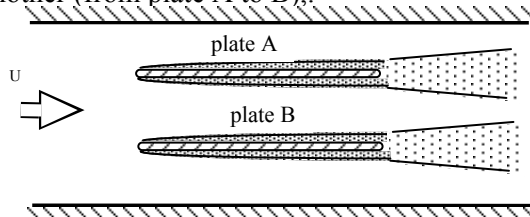


Figure 7: System of two plates

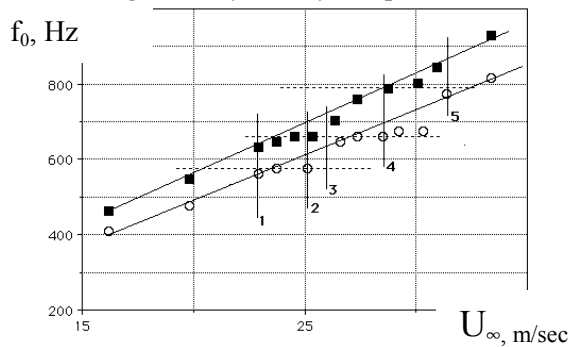


Figure 8: Coherent structures shedding frequency vs. free-stream velocity for two plates

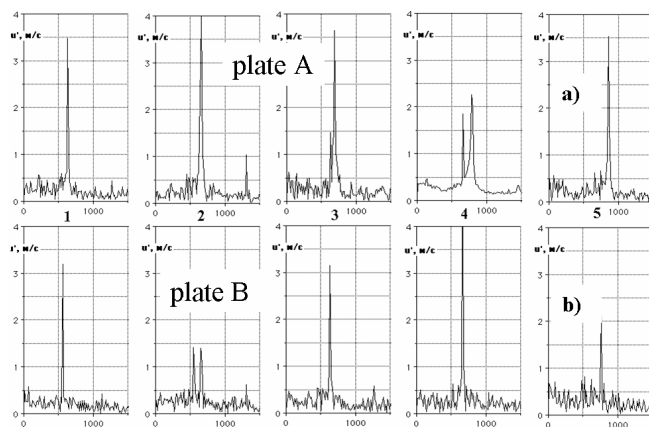


Figure 9: Spectra of velocity fluctuations in the wake behind the plates. a) plate A, b) plate B. 1),2),3),4),5)- velocity ranges shown on Figure 8

3.2 Axisymmetric case

The scheme of the experiment is presented at Figure 10. In difference with plane case the CS were of toroidal shape. Nevertheless, the integral parameter distributions were the same behind the trailing edge (Figure 11). The frequency of acoustic resonance can be defined from the data of Figure 12. (Note, that the same data exist for the plane case). If we look at the spectrum of velocity fluctuations behind the trailing edge for the second mode we discover the subharmonic $f_0/2$ origination (Figure 13), what is difference with the plane case. This oscillation starts from the separation zone as the fundamental frequency f_0 what was proved by the phase measurements presented at Figure 14. But the behavior of subharmonic is different - when the $f_0/2$ is maximum the f_0 is not (Figure 15).

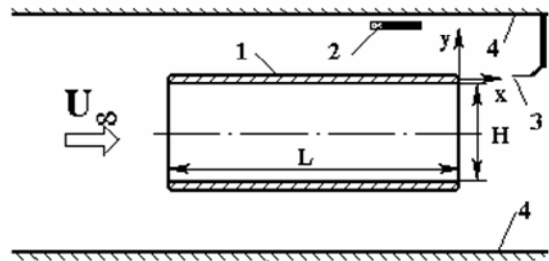


Figure 10: Experimental installation for tubes with thick walls

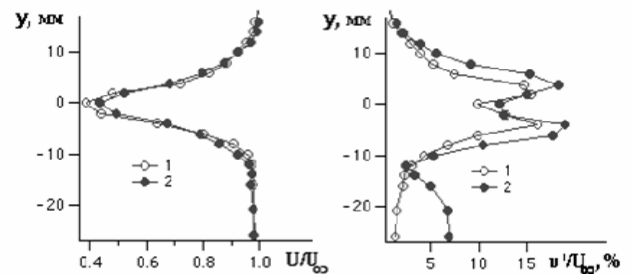


Figure 11: Mean velocity and rms velocity fluctuation distributions in the region of CS - 1 - nonresonant regime, 2 - resonant regime. $L=400$ mm, $x/d=1$

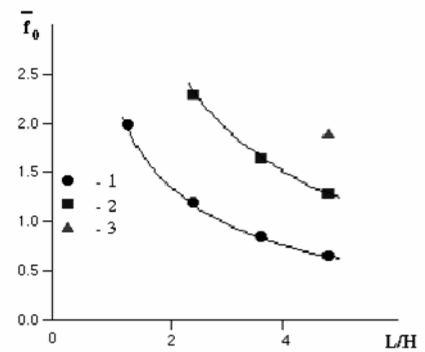


Figure 12: Acoustic resonance frequencies vs. length, 1, 2, 3 – first, second and third modes

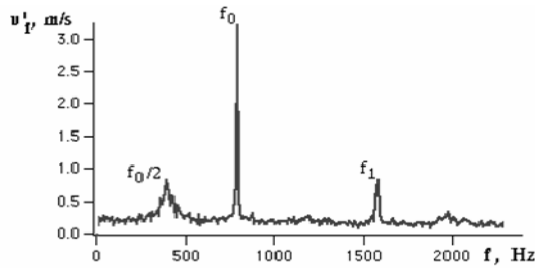


Figure 13: Spectrum of velocity fluctuations at the resonance. $L=400$ mm, $x/d=1$, second mode

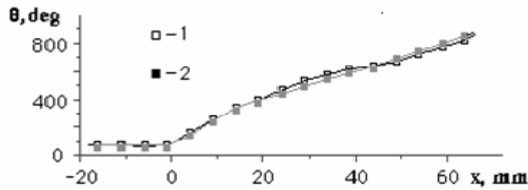


Figure 14: Phase of oscillations at frequency f_0 along streamwise coordinate at resonance conditions. Curves 1, 2 refer to upper and lower maximum, respectively. $L=400$ mm, first mode (see Fig. 12)

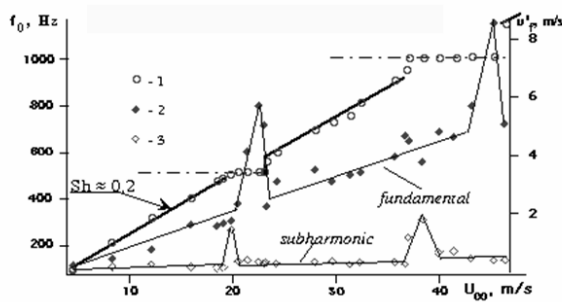


Figure 15: The frequency of fundamental and amplitude of fundamental and subharmonic vs. free-stream velocity

3.3 Bluff body - three-dimensional case

The round disk as a bluff body (Figure 16) was used as the model, with thickness $d = 8$ mm.

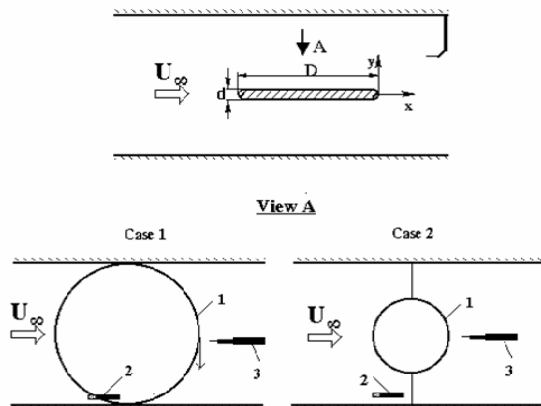


Figure 16: Scheme of experiment for 3D case. 1 – thick round disk, 2 – microphone, 3 – hot wire probe, 4 test section walls

3.3.1 CS development without resonance and with external excitation

At Figure 17 one can see the sample of velocity fluctuations spectrum behind the round disk for the case without resonance. Actually, the CS structures' frequency was the different for the different z -positions (Figure 18), and from this plot one can suspect the different growth rate in free-stream direction. But being excited by external loudspeaker the CS come to the same frequencies if the excitation frequency lies in receptivity range which is certain for each range of free-stream velocity (Figure 19).

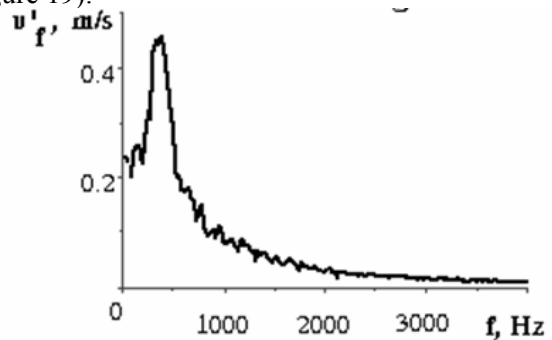


Figure 17: Spectrum of velocity fluctuations without resonance. $D = 200$ mm, $x/d=5$, $z/d=6$,

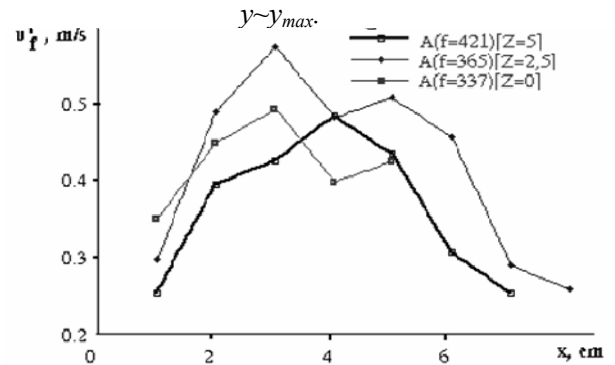


Figure 18: Velocity fluctuations of fundamental frequency in space at different spanwise z -locations, without resonance.

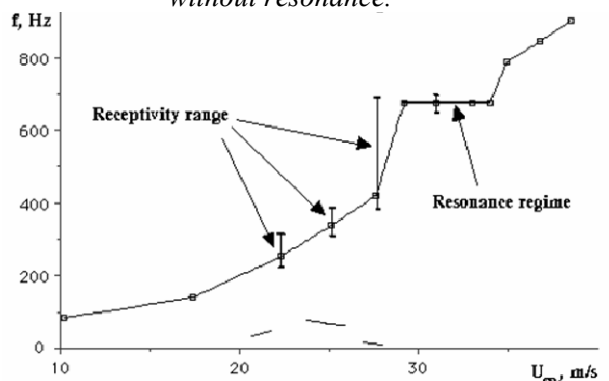


Figure 19: Natural frequencies and excitation by external loudspeaker. Vertical lines show the ranges of receptivity for different velocities

3.3.2 CS development at resonance regime

At resonance regime the CS spectrum contained many harmonics, so their development became strongly nonlinear, Figure 20. One can note that in difference with nonresonant regime the spectrum for the different spanwise locations contains the same components. As for the fundamental component, its phases lie at concentric circles (Figure 21).

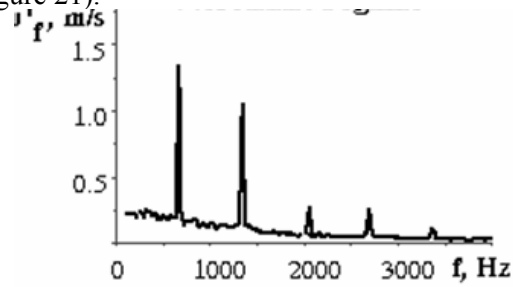


Figure 20: Spectrum of fluctuations, resonance regime. $D = 200$ mm, $x/d=3$, $z/d=0$, $y \sim y_{max}$.

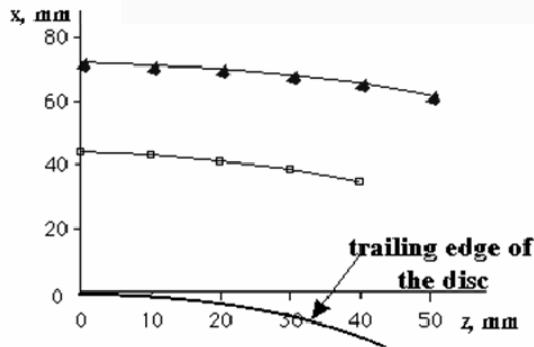


Figure 21: Lines of equal phase for fundamental frequency development in space, resonance regime.

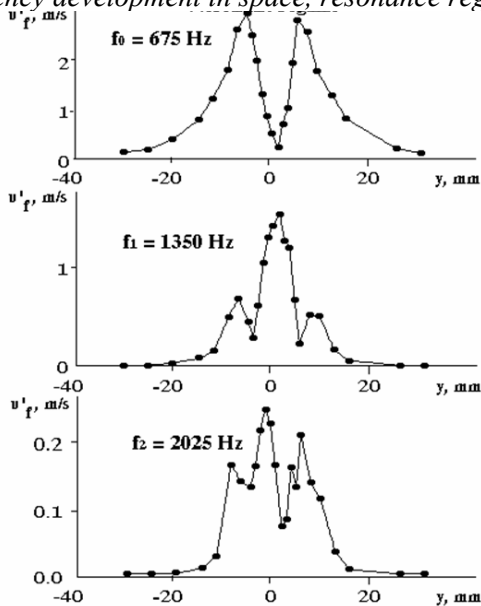


Figure 22: Distribution of spectral components, $D = 200$ mm, $x/d=3$, $z/d=0$.

Figure 22 shows the distribution of spectral components of velocity fluctuations in transversal direction. One can see that the maxima of them are located at different y -coordinates.

3.3.3 Sound wave and CS shape at resonance regime

By the hot-wire measurements the velocity distributions corresponding to sound wave were obtained. It was shown that their position in space coincided with the circle near the disk surface, and became more uniform far from the disk, Figure 23. So, the shape of sound wave was circular at the base, and transformed to square-like near the test section wall. The outline picture following from these results is presented at Figure 24.

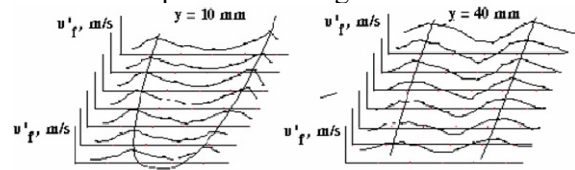


Figure 23: Sound wave distribution upright the disk at the different y -coordinate, $D = 160$ mm

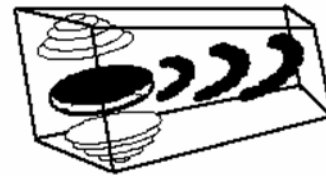


Figure 24: The sketch of sound wave shape and coherent structures position in near wake behind circular disk, $D = 160$ mm, resonance regime

3.4 Influence of trailing edge shape

The fine structure of flow at the wake origin in connection with resonance was analyzed. Examination of the power spectra revealed that, compared to the square leading edge, the semicircular leading edge provides better conditions for generating acoustic resonance by generating a more organized flow structure in the wake. The same is true for the rhombic trailing edge. In sum, of the different configurations considered by Katasonov et al, 2008, the configuration with a semicircular leading edge and a semicircular trailing edge was the best for generating aeroacoustic resonance.

4. CONCLUSION

Therefore, in this work complex of results about physical processes of onset and development of coherent structures had been obtained. The fundamental properties were studied of disturbances in wake. The relationship between flow characteristics around a plane, axisymmetrical and 3D bluff bodies in a duct and flow induced acoustic

resonance was studied experimentally. A hot-wire and a microphone were used to probe the flow and sound characteristics. When the sound frequency was synchronized with the vortex frequency near the trailing edge of plate, acoustic resonance occurred, i.e., the vortex shedding frequency remained constant as the free-stream flow velocity was increased further. We found that the shedding frequency measured by a hot-wire placed in the wake coincident with the sound frequency measured by a microphone inside the test section. Away from the resonances, the vortex shedding frequency increased linearly with increasing free-stream flow velocity. Few resonance modes were observed as the free-stream flow velocity was increased. When plotted as a function of f/f_0 and L/H , the resonance modes appeared as parallel hyperbolic curves. Furthermore, the wake structure behind the trailing edge under the resonance regime was well organized with a well-defined wake structure. The results can be used for flow optimization in various technological installations and for construction of theoretical models of the phenomena observed.

5. REFERENCES

Bardakhanov, S.P., Lygdenov, V.Ts., 1990, Coherent structures in the wake behind a bluff body and generation of sound under resonant conditions. *Izv. Sib. Otd. Akad. Nauk SSSR, Ser. Tekh. Nauk*, 2, 36-40.

Katasonov, M.M., Sung, H.J., Bardakhanov, S.P., 2008, Wake flow-induced acoustic resonance around a long flat plate in a duct (in press).

Parker, R. 1966, Resonance effects in wake shedding from parallel plates: some experimental observations. *J. Sound Vibr.*, 4, 1, 62-72.

Sukhinin, S.V., Bardakhanov, S.P., 1998, Aeolian tones of a plate in a channel. *Prikl. Mekh. Tekh. Fiz.*, 39, 2, 69-77.